

The nanocrystalline cellulose from *Ananas comosus* leaf wastes: An overview to extraction, purification, and applications as curcumin drug delivery system

Sumaiyah Sumaiyah^{1*}, Poppy Anjelisa Zaitun Hasibuan², Hafid Syahputra³, Muhammad Fauzan Lubis⁴

¹Department of Pharmaceutical Technology, Faculty of Pharmacy, Universitas Sumatera Utara, Medan, Indonesia.

²Department of Pharmacology, Faculty of Pharmacy, Universitas Sumatera Utara, Medan Indonesia.

³Department of Pharmaceutical Chemistry, Faculty of Pharmacy, Universitas Sumatera Utara, Medan, Indonesia.

⁴Department of Pharmaceutical Biology, Faculty of Pharmacy, Universitas Sumatera Utara, Medan Indonesia.

ARTICLE HISTORY

Received on: 28/05/2024
Accepted on: 20/09/2024
Available Online: 05/11/2024

Key words:

Ananas comosus,
nanocrystall cellulose,
curcumin, non-Fickian,
antimicrobial activity.

ABSTRACT

Currently, antibacterial materials are attracting considerable attention across various fields. In this study, curcumin (Cur) was prepared with nanocrystal cellulose (NCC) into the polyvinyl alcohol (PVA) matrix to improve the functional properties of a pure Cur-NCC-PVA film. The NCC was obtained from *Ananas comosus* leaves and characterized by Fourier transform infrared (FTIR), scanning electron microscope (SEM), X-ray diffraction (XRD), and particle size analysis. The variations of Cur concentrations (50, 75, and 100 µg) were added to prepare Cur-NCC-PVA films. The release kinetics of Cur from the films was determined using a spectrophotometer and the release kinetic model was obtained using Korsmeyer-Peppas kinetic model. The antibacterial activity of Cur-NCC-PVA films was established using the diffusion method. The results of NCC characteristics showed satisfactory significance. The FTIR showed a functional group of chemical composition that confirmed the removal of non-cellulosic constituents. XRD confirmed the crystallinity index of NCC of 75.89%. Meanwhile, the particle size of NCC of 268.45 nm. The development of Cur-NCC-PVA films showed a uniform yellow color. The release of curcumin in all films was increased depending on the time following the zero-order kinetic reaction. The non-Fickian kinetics demonstrated the mechanism of Cur release from the film. The Cur-NCC-PVA films in Cur concentration of 100 µg were confirmed to have the highest antibacterial activity and significantly different between 50 and 75 µg Cur-NCC-PVA films against *Bacillus subtilis*, *Streptococcus spp.*, and *Escherichia coli*. The Cur-NCC-PVA films described the potential activity for topical formulation in skin disease treatment.

INTRODUCTION

In recent years, a few films have undergone rapid development, particularly films that inhibit the growth of microorganisms [1]. When making antimicrobial films, it is common practice to incorporate antimicrobial materials such as silver nanoparticles [2], zinc oxide, copper oxide, titanium dioxide [3], organic acids (benzoic acid and sorbates) [4], enzymes (lysozyme and glucose oxidase) [5], natural active compounds (essential oil, biopolymer, and curcumin (Cur)

[6], antibiotics, triclosan, and other functional. In addition to this, several researchers have developed composite materials that have many functions, including antibacterial action and antioxidant activity [7–10].

Cur [1,7-bis(4-hydroxy-3-methoxyphenyl)-1,6-heptadiene-3,5-dione] is a type of polyphenolic phytoconstituent that may be found in the rhizomes of *Curcuma longa* (turmeric) [11,12]. It has properties that make it effective against cancer [13], inflammation [14], bacteria [15], and antioxidants [16]. For thousands of years, turmeric has been used both as a seasoning and as a natural herbal remedy in traditional medicine [17]. Due to the presence of many phenolic hydroxyl groups along the chain of the molecule, the Cur that is derived from turmeric has the capacity to scavenge reactive oxygen species, which speeds up the process of wound healing [18,19]. Even when

*Corresponding Author
Sumaiyah Sumaiyah, Department of Pharmaceutical Technology, Faculty of Pharmacy, Universitas Sumatera Utara, Medan, Indonesia.
E-mail: sumaiyah@usu.ac.id

administered to people at high levels (twelve grams per day), Cur was found to be safe as a treatment in clinical trials [20].

In the previous research reported by [21] the Cur–chitosan (Cur–CH) blend films were developed by using the technique of solution casting. This Cur–CH blend films that resulted exhibited outstanding tensile strength as well as antibacterial activity against *Staphylococcus aureus* and *Rhizoctonia solani* [21]. Ionic liquid (1-allyl-3-methyl-imidazolium chloride) was used as the solvent to prepare cellulose/Cur composite films. The composite films that included Cur displayed good mechanical qualities, thermal stability, and anti-bacterial activity, all of which could have potential applications in the sectors of food packaging and medicine [22]. In addition, [23] developed a straightforward solvent-casting method to create *C. longa* oil-loaded polyacrylonitrile (PAN) films. The hydrophilicity of the films was increased as a result of the incorporation of oil from *C. longa* into the PAN matrix [23]. A methoxy poly (ethylene glycol)-graft-chitosan film coated with Cur nanoformulation was also developed (Cur–MPEG–chitosan film). According to the results of the *in vivo* wound healing test, the Cur–MPEG–chitosan film successfully promoted wound healing [24].

The material known as nanocellulose is derived from cellulose that can be found in a wide variety of natural sources, including plants, animals, algae, fungi, and bacteria [25]. Cellulose is one of the most common types of polymer found in the world. Cellulose itself is a fascinating and versatile biopolymer that consists of linear, covalently linked chains of D-glucose units [26]. In addition to this, it is a substance that can be broken down by natural processes and is one of the biopolymers that are sustainable in nature [27]. These days, there is a lot of interest in both the synthesis of it and its use as a polymer in the production of biomaterials [28,29]. Nanosized materials have a high homogeneity of crystalline morphology, a wide surface area, and better mechanical capabilities; as a result, there is a growing trend toward employing nanosized materials in modern-day applications [30,31]. In previous studies, nanocellulose has been used as a carrier for treating various types of diseases. For instance, Zikmundova *et al.*, reported that bacterial nanocellulose loaded with Cur exhibited more antibacterial activity than pristine nanocellulose [32]. In addition, Gunathilake *et al.*, revealed the effect of Cur-loaded nanocellulose as an antiviral [33]. Nevertheless, the characteristic of Cur is poorly water-soluble causing the lack of Cur delivery from the nanocellulose films [34].

Therefore, in this study, polyvinyl alcohol (PVA) was used to increase the solubility of Cur. PVA is used because it contains hydroxyl and acetyl groups which are able to form the PVA structure into micelles in aqueous media and facilitate increased solubility of Cur [35]. When the solubility of Cur experiences a significant increase, it will increase the amount of Cur that enters the nanocellulose [36]. Increasing Cur loading in nanocellulose will be very promising for development in the health sector.

MATERIALS AND METHODS

Preparation of nanocrystalline cellulose

A modified procedure produced nanocrystal cellulose (NCC). Briefly, α -cellulose from *Ananas comosus* (L) Merr.

leaf (40.0 g) was hydrolyzed in 40% w/w sulfuric acid at 45 °C and swirled at high speed for 25 minutes. After dilution, the cellulose suspension settled overnight. The clear top layer was decanted and the white hazy layer was washed with deionized water and centrifuged three times to remove most soluble cellulose. The thick, white suspension was dialyzed against slow-flowing distilled water for 1–4 days using dialysis tubing with a 12,000–14,000 molecular weight cutoff (Spectra/Por[®], Spectrum Laboratories, Inc, Rancho Dominguez, CA, USA). Ultrasound therapy in a Fisher Sonic Dismembrator (Fisher Scientific, Ottawa, ON, Canada) for 10 minutes at 60% power dispersed dialysis tube suspension [37-39].

Characterization of nanocrystalline cellulose

Fourier transform infrared (FTIR) analysis

Functional group investigations used FTIR spectrometers (Shimadzu, Kyoto, Japan). Investigated functional group changes at different wavelengths. An attenuated total reflection FTIR (ATR-FTIR) spectrograph with 34 scans and 4 cm⁻¹ spectral resolution spanning 500–4000 cm⁻¹ was used to obtain the FTIR spectra [40].

Morphological analysis

The Scanning Electron Microscope (SEM) was used to observe NCC morphologies. Sample surface morphology was examined using a 1.0 kV JEOL/EO SEM (Hitachi TM3030, JEOL, Ltd., Tokyo, Japan). The sample was sputter-coated with Pt at 15 mA for 20 s to avoid charging [41].

X-ray diffraction (XRD)

The sample was examined using Cu K radiation at 40 kV, 30 mA, and 0.15 mm receiving slit using D-MAX 2200 VPC (Rigaku Ltd., Japan). Reflection intensity was measured at 2°/min with a scan range of 10–80. According to Hamad and Hu calculated crystallinity from x-ray intensity [42].

Particle size analysis

The particle size of NCC was determined using a particle size analyzer (PSA) (Analysette 22 NanoTec, FRITSCH Ltd., Germany) [43].

Development of curcumin finishing NCC-PVA film

Film preparation

Films were prepared by a previously reported method with modification. Briefly, 0.3 g of PVA, is put in a beaker glass containing 10 mL of distilled water, dissolved using a hot plate stirrer at 80°C. After complete dissolution, 0.3 g of NCC was added and 50 μ g, 75 μ g, and 100 μ g of Cur were added, respectively. Ultrasonication at 80% amplitude for 20 min followed by 2 h of stirring at 80°C. Pouring the liquids on a petri dish and letting them dry at room temperature produced a film [44].

Study of release kinetics of curcumin

At 1:100 (w/v), cellulose nanocrystal films were added to conical flasks containing artificial sweat solution (Sodium chloride 5 g/L, Urea 1 g/L, lactic acid 1 g/L; adjusted to pH 5.5 with 1 M sodium hydroxide). At 37 °C and 80 rpm,

the samples were orbital shaken. At the predetermined period (0, 2, 4, 6, 8, 10, 12, 18, 24, 36, and 48 h), a flask was extracted and spectrophotometer absorbance was measured at 460 nm (Shidmazu). Using Cur standard curves, the film's Cur was calculated (Sigma). In this study, the Cur-PVA film without NCC was prepared as a control [45].

Antibacterial activity of curcumin-NCC-PVA Films

The antibacterial activity of the Cur-NCC-PVA film was determined using the diffusion method. In summary, 100 μ L of bacterial suspension (*Bacillus subtilis*, *Streptococcus sp.*, *Escherichia coli*) was placed in 15 mL of Mueller Hinton Agar (MHA) and then left to harden. At the same time, a 6 mm Cur-NCC-PVA film was placed on the surface and incubated for 24 h, 37 °C. The clear zone formed around the Cur-NCC-PVA film was observed and measured. The clear zone contains the antibacterial activity of the Cur-NCC-PVA film. Gentamicin was used as a positive control, while NCC-PVA film without Cur was used as a negative control [46].

Analysis data

Antimicrobial activity data were processed using Microsoft Excel 2020. The data were tested using One Way Anova (ANOVA) and continued with the Tukey HSD Test using SPSS 22 (SPSS, Inc.; IBM Corp.; Chicago, IL, USA). All data are presented in $n = 3 \pm$ standard deviation (SD). The data expressed a significant difference with $p < 0.05$.

RESULTS

Characterization of nanocrystalline cellulose

In this study, the preparation of nanocrystalline cellulose (NCC) from *A. comosus* leaves was obtained using the acid hydrolysis method in the concentration of sulfuric acid used is 40%. 3.81 g white powder (NCC) was obtained from 5 g α -cellulose (Fig. 1). Some tests were conducted to determine the quality of NCC. The group function of NCC was carried out using FT-IR with avicel as compared material. Figure 2 shows the FT-IR spectrum of samples. Avicel and NCC have the same spectra as shown in Figure 2. The characteristic peaks of NCC are at 3375 (O–H stretching), 2908 (C–H stretching) [47], 1635 (OH from water absorption), and 1060 cm^{-1} (C–O stretching from glycoside bond) [48].

The surface structure of NCC is shown in Figure 3A with a magnification of 50,000. The SEM micrograph of the NCC suspension shows individual NCC fibers with approximate dimensions of 100 μ m wide. The structure and index of crystallinity of NCC were analyzed by XRD. Figure 3B shows that the index of crystallinity NCC is 75.89% which is indicated by the sharp peaks of the spectrum of NCC. The resulting NCC has an average particle size of 268.45 nm which can be seen in Figure 3C.

Characterization of nano cellulose film: release kinetic

Cur-NCC films were obtained using PVA as a binder and film-maker for its excellent combination of physical as well as chemical characteristics including good solubility in water, affinity to complex materials, film-forming capability, nontoxicity, biocompatibility, and biodegradability [49]. The

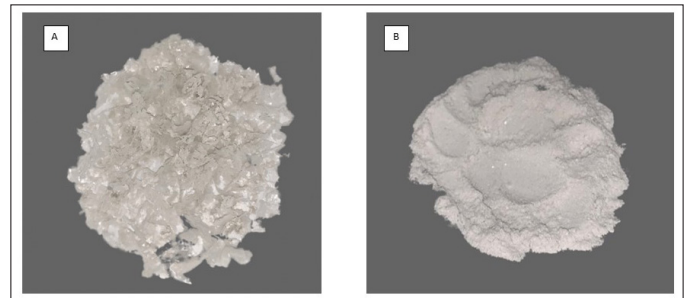


Figure 1. Nanocrystalline cellulose from *A. comosus* leaves (A) before the powder is crushed and (B) after the powder is crushed.

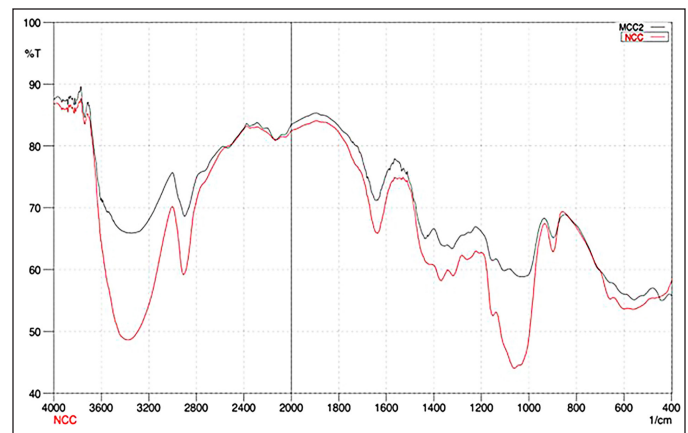


Figure 2. Infrared spectra of (-) avicel and (-) nanocrystalline cellulose.

variations (50, 75, and 100 μ g) concentration of Cur were added to the formula. The PVA will enhance the solubility of Cur causing the Cur absorption into NCC will increase. In addition, the presence of PVA in this film will provide good mechanical strength, flexibility, and adhesion properties of the film. The films are formed due to the formation of hydrogen bonds between NCC and PVA [50]. The developed films display a homogenous lattice with yellowish and slightly opaque (Fig. 4). The release of Cur from the NCC-PVA film was evaluated in skin temperature for a duration of 48 hours (Fig. 5). Figure 5 shows Cur release of Cur-NCC-PVA films was increased with time dependent. The release of Cur from each NCC-PVA film (50, 75, and 100 μ g of Cur-loaded NCC-PVA film) following zero-order kinetic reaction with R^2 values of 0.98, 0.97, and 0.99, respectively. Examining kinetic data using different kinetic models provides insight into the mechanism of drug release. The drug release kinetics in this study were assessed using the widely recognized Korsmeyer–Peppas kinetic model. The non-Fickian diffusion demonstrated the mechanism of Cur release with the value of release exponent 0.21, 0.22, and 0.19, respectively [51].

In the context of a Cur-NCC-PVA film, the non-Fickian diffusion model refers to the mechanism of diffusion of Cur molecules within the film matrix, which deviates from the classical Fickian diffusion behavior [52]. The non-Fickian diffusion model in Cur-NCC-PVA films suggests that the diffusion of Cur molecules is influenced

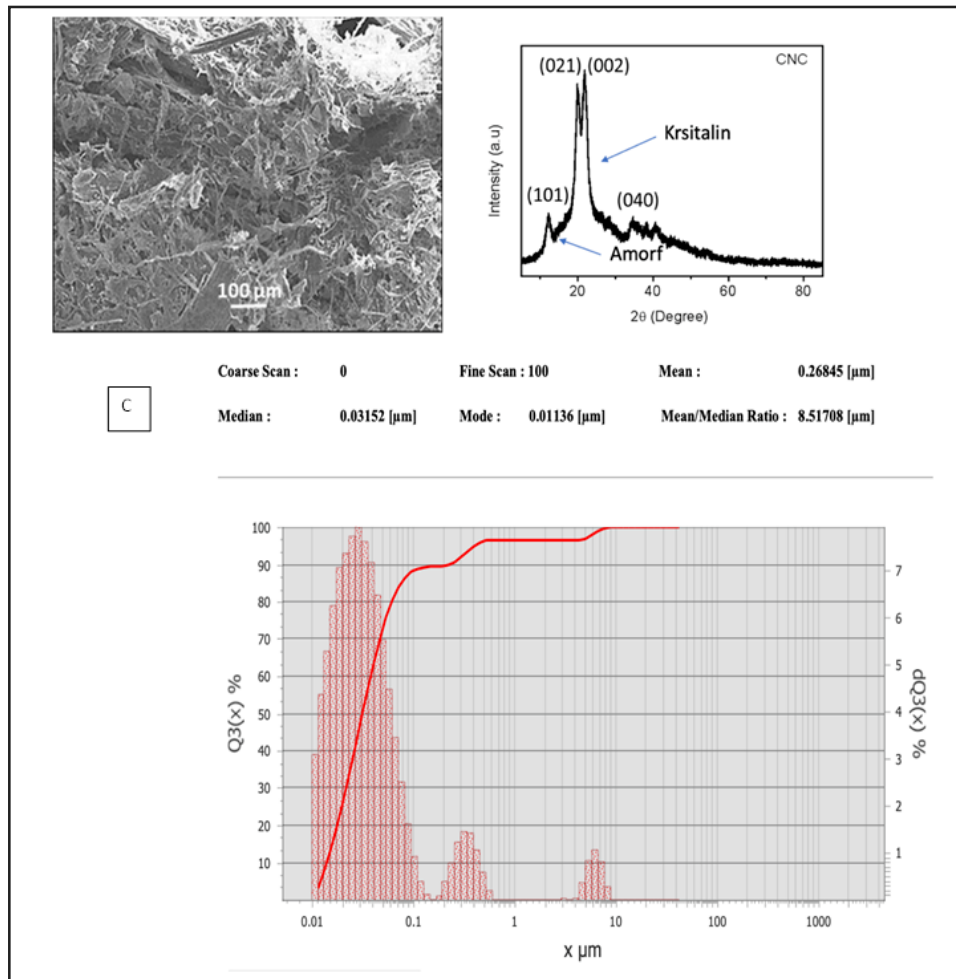


Figure 3. Morphological structure, index crystallinity, and particle size of nanocrystall cellulose, (A) SEM, (B) X-ray, and (C) particle size.

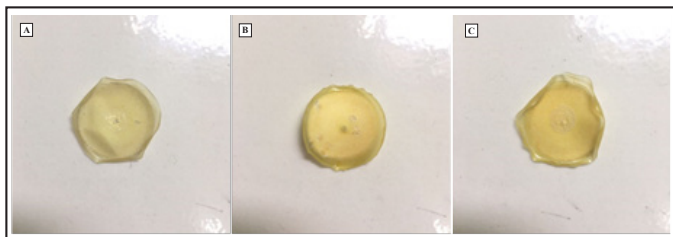


Figure 4. Cur-NCC-PVA films, (A) 50 μg Cur-NCC-PVA film, (B) 75 μg Cur-NCC-PVA film, and (C) 100 μg Cur-NCC-PVA film.

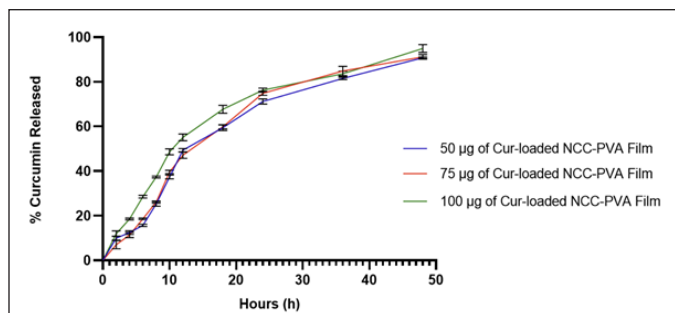


Figure 5. Release of the curcumin from NCC-PVA film.

by factors beyond the simple concentration gradient, such as interactions between Cur and the polymer matrix (NCC and PVA), as well as the film's structural properties [53]. These interactions can affect the rate and extent of Cur release from the film. Understanding and modeling non-Fickian diffusion in Cur-NCC-PVA films are crucial for optimizing their performance in applications such as controlled drug delivery or active packaging [54].

The release of Cur from the NCC-PVA film formulation in this study is consistent with what has been described in previous research. As reported by Zhu *et al.* [55], tetracycline hydrochloride from the NCC-PVA film formulation exhibits zero-order model release with an R^2 value of 0.99. A similar phenomenon was described by Kolakovic *et al.* [56], where the zero-order model describes the release of itraconazole and beclomethasone from NCC materials. This suggests that some drugs will be entrapped within the NCC. Additional polymers such as PVA are needed to coat the drug binding and NCC. Generally, it is explained that these films will be swelling when subjected to stimuli such as pH or temperature. Film swelling leads to the release of Cur from NCC [57,58].

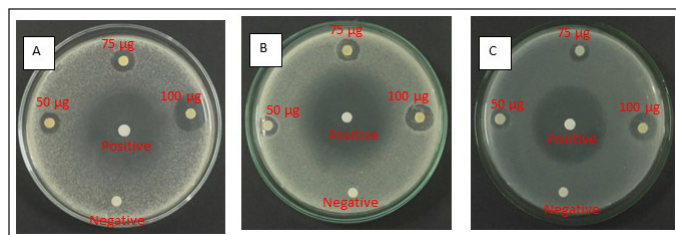


Figure 6. Antimicrobial activity of Cur-NCC-PVA films against pathogenic microbial, (A) *B. Subtilis*, (B) *Streptococcus sp.*, and (C) *E. coli*.

Table 1. Diameter of clear zone (mm) after treatment with Cur-NCC-PVA films.

Sample	*Diameter of clear zone (mm) \pm SD		
	<i>B. subtilis</i>	<i>Streptococcus sp.</i>	<i>E. coli</i>
Negative control	-	-	-
Positive control	34.20 \pm 1.05	31.15 \pm 1.10	32.10 \pm 1.12
50 μ g Cur-NCC-PVA film	9.17 \pm 0.95	8.12 \pm 0.60	12.71 \pm 0.74
75 μ g Cur-NCC-PVA film	12.53 \pm 1.00	9.50 \pm 0.80	9.85 \pm 0.92
100 μ g Cur-NCC-PVA film	18.85 \pm 1.10 ^{ab}	16.25 \pm 1.08 ^{ab}	15.30 \pm 1.02 ^{ab}

*Diameter of clear zone (mm) is significantly different with $p < 0.05$ ($n = 3 \pm$ SD).

^a100 μ g Cur-NCC-PVA film is significantly different with 50 μ g Cur-NCC-PVA film ($p < 0.05$).

^b100 μ g Cur-NCC-PVA film is significantly different with 75 μ g Cur-NCC-PVA film ($p < 0.05$).

Antimicrobial efficacy of curcumin-nanocrystalline cellulose film

The antimicrobial activity of Cur-NCC-PVA films was obtained using the diffusion method as per AATCC 147 against *B. subtilis*, *Streptococcus sp.*, and *E. coli* [59]. The nanocellulose film without the addition of Cur was used as the negative control and gentamicine as a positive control. The antimicrobial activity of Cur-NCC-PVA films can be shown in Figure 6. The antibacterial activity of Cur-NCC-PVA films was determined by measuring the clear zone around the film [60]. Hereinafter referred to as the inhibition zone. The results of the inhibition zone can be seen in Table 1.

The Cur content in the film affects its antibacterial activity (Table 1). The 100 μ g Cur-NCC-PVA films have the highest activity against *B. subtilis*, *Streptococcus sp.*, and *E. coli* than 50 μ g Cur-NCC-PVA films and 75 μ g Cur-NCC-PVA films ($p < 0.05$). However, the activity was still lower than the positive control (Gentamicine).

DISCUSSION

During this research, NCC was extracted from the leaves of *A. comosus*. Reported *A. comosus* leaves have a significant cellulose content [61]. After the pineapples have been harvested in Indonesia, the *A. comosus* leaves are the part of the plant that is thrown away. To create a source of natural materials that are not being exploited, the leaves will be used

[62]. It is possible to include the NCC that was produced during acid hydrolysis in the drug delivery process and use it as an addition [63]. The leaves of the *A. comosus* are not the main source of NCC. NCC can be produced from a wide variety of naturally occurring sources, and these can all serve as potential sources [64]. Nevertheless, the quality of the NCC will vary depending on the sources used. As a result, the quality of the isolated NCC was characterized in this study to ensure that it is suitable for use as a medication additive.

The most well-known and often employed approach to the production of NCC is called acid hydrolysis. Single crystals are liberated as a byproduct of this process, which deconstructs the disordered and amorphous cellulose moieties [65]. The formation of colloidal particles occurs when, during the acid hydrolysis process, sulfate groups take the place of hydroxyl groups. The presence of these groups on the surface of the cellulose helps to maintain the particles' state of suspension [66]. Hydrolysis of cellulose was accomplished at an acid concentration of 40% sulfuric. After processing 5.0 g of cellulose, a total of 3.81 g of NCC was produced. The NCC that was produced was in the shape of crystals that were white in color. This is consistent with what was found in earlier investigations and confirms their findings [67,68]. When carrying out this procedure, it is essential to consider the concentration of the acid. Because of the acid's incapacity to hydrolyze beta-cellulose, the concentration of the acid must be high enough [69]. However, if the concentration of the acid is too high, this will result in the material's complete deterioration. When cellulose is burned, it is converted into carbon, which may be identified by the transformation of the suspension's color to a solid black and by the black powder that is produced, which is the color that is characteristic of carbon [70,71].

The FT-IR was then used to continue the identification of the NCC. The NCC possesses a few functional groups that can be employed in the identification process [72]. These groups include OH, C-H, OH derived from water absorption, and C-O (Fig. 2). The presence of the OH group at 1635 cm^{-1} suggests that the resulting product is NCC, which is also present in Avicel. This substance can be identified by its molecular formula [73]. The microcrystalline cellulose known as Avicel is the standard against which the FT-IR spectral pattern of NCC is measured. The acid hydrolysis process involves the absorption of water, which results in the sharp peak of the OH absorption line in the spectrum. This functional group does not belong to the lignin or the hemicellulose components, which enables the NCC to classify it as a typical group [74]. The cellulose crystal diffraction pattern peaks can be seen in Figure 3B. These peaks are located around $2\theta = 15.4^\circ$ and 22.3° . According to the data found in JCPDS 50-2241, the diffraction of cellulose occurs at angles of $2\theta = 15.0^\circ$ and 22.8° . This diffraction peak agrees with those findings [75,76]. To determine the crystallinity, the Segal method was utilized, and the final NCC value came out to be 75.89% [77]. Crystallinity in NCC can be quantitatively analyzed using the crystallinity index, which offers information that can be related to the fibers' strength and stiffness [78]. When compared to low crystallinity, high crystallinity suggests an organized molecular structure, which indicates small particles. The low

crystallinity, on the other hand, shows that the structure is more disordered, which results in an amorphous powder [79]. The findings regarding the particle size lend credence to the crystallinity characterization of the sample that was collected, which was found to be 268.45 nm (Fig. 3C).

According to the previous study, the visual examination of the micrograph reveals substantial morphological similarities with NCC (Fig. 3A) [80]. NCC is a hydrophilic crystalline biopolymer that possesses nanoscale dimensions in addition to renewability and a large surface area. To create nanocomposite materials, NCC is frequently combined with a diverse array of polymeric matrices [81]. The Cur-NCC-PVA films were acquired for the purpose of this study. The produced film has a golden hue that is consistent throughout and has a thickness of 0.4 mm (Fig. 4). Even with a relatively low filler loading, the films' mechanical characteristics were significantly enhanced using PVA as the polymer matrix [82]. In addition to this, the polymeric matrix influences the drug release kinetics emanating from the film [83,84]. At a temperature comparable to that of the skin, a period of 48 hours was spent monitoring the rate of Cur release from the NCC-PVA films (Fig. 5). The model that was employed is a well-known tool for researching the kinetics of drug release for topical formulations [85]. During the test, there was no evidence of a burst release effect. The release of Cur achieves plateau conditions after 48 hours, with a total release of $90.81\% \pm 0.30\%$; $91.23\% \pm 0.87\%$; and $94.96\% \pm 1.43\%$ from each NCC-PVA film. It does this by releasing the medicine at a steady rate to keep the drug level at a therapeutically effective threshold. The nanocrystals of cellulose in the film act as a barrier to diffusion, which slows the burst release action of Cur from the film [86]. For the films to have an antibacterial action that is effective over the long term, the control release property is necessary and this study presented that [87].

Antimicrobial activity was observed throughout a broad spectrum in the film that included Cur [88]. Two Gram-positive bacteria and one Gram-negative bacteria were significantly inhibited by the film's considerable inhibitory action (Table 1). To provide a negative control, a cellulose nanocrystal film was utilized that had no Cur finishing applied to it. Based on the findings, it was determined that the control films did not demonstrate any inhibitory impact on any of the microorganisms that were tested. The presence of a clear zone around the films provided evidence of the developed film's ability to inhibit the growth of microorganisms [89]. Based on these findings, the size of the clear zone was greater whenever there were larger concentrations of Cur in the film. On *B. subtilis*, the inhibition zone produced by 100 µg of Cur-NCC-PVA film was found to have the greatest observed size ($p < 0.05$). Antibacterial activity was demonstrated by this film against *Streptococcus sp.* and *E. coli*, with clear zones of 16.25 ± 1.08 and 15.30 ± 1.02 mm, respectively ($p < 0.05$). As an antibacterial agent, Cur has been the subject of a significant amount of research and testing. It was shown that Cur prevented *B. subtilis* from going through the cytokinesis process by inducing filamentation. Additionally, it strongly inhibited the production of cytokinetic Z-rings in *B. subtilis* without having

a major impact on the segregation and organization of the nucleoids [90,91]. The research conducted on *E. coli* and *B. subtilis* showed that Cur, due to its inhibitory impact against FtsZ polymerization, could block the FtsZ assembly, which in turn disrupts prokaryotic cell division [92,93]. In conclusion, the results of this research showed that Cur-NCC-PVA films possess antibacterial action. The production of this film is an intriguing study of the topical use of Cur, and the usage of Cur-NCC-PVA films can be used to treat a variety of illnesses that are associated with skin infections.

CONCLUSION

Ananas comosus leaves can provide NCC, which can serve as a carrier for Cur in film processes. The film's controlled release of Cur followed a zero-order reaction, which is a beneficial characteristic for its topical application. The antibacterial activity of the Cur-NCC-PVA films against *B. subtilis*, *Streptococcus sp.*, and *E. coli* further supports this claim. Moreover, the film that contains 100 µg of Cur demonstrates promising promise as a therapy for wounds. Optimization of the film recipe is necessary to enhance the clarity and measurability of the Cur release mechanism. This will facilitate the utilization of this film as a topical formulation in the skin health sector.

LIST OF ABBREVIATIONS

CH: chitosan; Cur: curcumin; FTIR: Fourier transform infrared; NCC: nanocrystalline cellulose; PSA: particle size analyzer; PVA: polyvinyl alcohol; SEM: scanning electron microscope; XRD: X-ray diffraction.

ACKNOWLEDGEMENTS

The authors thank the Universitas Sumatera Utara for providing the facilities to finish this work.

AUTHOR CONTRIBUTIONS

All authors made substantial contributions to conception and design, acquisition of data, or analysis and interpretation of data; took part in drafting the article or revising it critically for important intellectual content; agreed to submit to the current journal; gave final approval of the version to be published; and agree to be accountable for all aspects of the work. All the authors are eligible to be an author as per the International Committee of Medical Journal Editors (ICMJE) requirements/guidelines.

FINANCIAL SUPPORT

This work accepts funding from Universitas Sumatera Utara via the TALENTA scheme 2021 with contract No. 234/UN5.2.3.1/PPM/SSP-TALENTA USU/2021.

CONFLICTS OF INTEREST

The authors report no financial or any other conflicts of interest in this work.

ETHICAL APPROVALS

This study does not involve experiments on animals or human subjects.

DATA AVAILABILITY

All data generated and analyzed are included in this research article.

PUBLISHER'S NOTE

All claims expressed in this article are solely those of the authors and do not necessarily represent those of the publisher, the editors and the reviewers. This journal remains neutral with regard to jurisdictional claims in published institutional affiliation.

USE OF ARTIFICIAL INTELLIGENCE (AI)-ASSISTED TECHNOLOGY

The authors declares that they have not used artificial intelligence (AI)-tools for writing and editing of the manuscript, and no images were manipulated using AI.

REFERENCES

- Galiano F, Mancuso R, Guzzo MG, Lucente F, Gukelberger E, Losso MA, *et al.* New polymeric films with antibacterial activity obtained by UV-induced copolymerization of acryloyloxyalkyltriethylammonium salts with 2-hydroethyl methacrylate. *Int J Mol Sci.* 2019;20(11):1–11.
- Hegazy MA, Borham E. Preparation and characterization of silver nanoparticles homogenous thin films. *NRIAG J Astron Geophys.* 2018;7(1):27–30. doi: <https://doi.org/10.1016/j.nrjag.2018.04.002>
- Oun AA, Shankar S, Rhim JW. Multifunctional nanocellulose/metal and metal oxide nanoparticle hybrid nanomaterials. *Crit Rev Food Sci Nutr.* 2020;60(3):435–60. doi: <https://doi.org/10.1080/10408398.2018.1536966>
- Suganthi S, Vignesh S, Kalyana Sundar J, Raj V. Fabrication of PVA polymer films with improved antibacterial activity by finetuning via organic acids for food packaging applications. *Appl Water Sci.* 2020;10(4):1–11. doi: <https://doi.org/10.1007/s13201-020-1162-y>
- Hibbard HAJ, Reynolds MM. Enzyme-activated nitric oxide-releasing composite material for antibacterial activity against *Escherichia coli*. *ACS Appl Bio Mater.* 2020;3(8):5367–74.
- do Evangelho JA, da Silva Dannenberg G, Biduski B, el Halal SLM, Kringel DH, Gularte MA, *et al.* Antibacterial activity, optical, mechanical, and barrier properties of corn starch films containing orange essential oil. *Carbohydr Polym.* 2019;222:114981. doi: <https://doi.org/10.1016/j.carbpol.2019.114981>
- Li J, Zhuang S. Antibacterial activity of chitosan and its derivatives and their interaction mechanism with bacteria: Current state and perspectives. *Eur Polym J.* 2020;138:109984. doi: <https://doi.org/10.1016/j.eurpolymj.2020.109984>
- Rhim JW, Wang LF, Hong SI. Preparation and characterization of agar/silver nanoparticles composite films with antimicrobial activity. *Food Hydrocoll.* 2013;33(2):327–35.
- Priya B, Gupta VK, Pathania D, Singha AS. Synthesis, characterization and antibacterial activity of biodegradable starch/PVA composite films reinforced with cellulosic fibre. *Carbohydrate Polym.* 2014;109:171–9.
- Wang Y, Guo X, Pan R, Han D, Chen T, Geng Z, *et al.* Electrodeposition of chitosan/gelatin/nanosilver: a new method for constructing biopolymer/nanoparticle composite films with conductivity and antibacterial activity. *Mater Sci Eng C.* 2015;53:222–8.
- Kocaadam B, Şanlıer N. Curcumin, an active component of turmeric (*Curcuma longa*), and its effects on health. *Crit Rev Food Sci Nutr.* 2017;57(13):2889–95.
- Nugraha SE, Laila L, Satria D, Syahputra RA. HPTLC analysis of *Curcuma mangga* val. Extracts and their immunomodulatory effects on delayed-type hypersensitivity response. *Rasayan J Chem.* 2021;14(3):2085–9.
- Tomeh MA, Hadianamrei R, Zhao X. A review of curcumin and its derivatives as anticancer agents. *Int J Mol Sci.* 2019;20(5):1033.
- Edwards RL, Luis PB, Varuzza PV, Joseph AI, Presley SH, Chaturvedi R, *et al.* The anti-inflammatory activity of curcumin is mediated by its oxidative metabolites. *J Biol Chem.* 2017;292(52):21243–52. doi: <http://dx.doi.org/10.1074/jbc.RA117.000123>
- Izui S, Sekine S, Maeda K, Kuboniwa M, Takada A, Amano A, *et al.* Antibacterial activity of curcumin against periodontopathic bacteria. *J Periodontol.* 2016;87(1):83–90.
- Chen X, Zou LQ, Niu J, Liu W, Peng SF, Liu CM. The stability, sustained release and cellular antioxidant activity of curcumin nanoliposomes. *Molecules.* 2015;20(8):14293–311.
- Akbar MU, Rehman K, Zia KM, Qadir MI, Akash MSH, Ibrahim M. Critical review on curcumin as a therapeutic agent: from traditional herbal medicine to an ideal therapeutic agent. *Crit Rev Eukaryot Gene Expr.* 2018;28(1):17–24.
- Krausz AE, Adler BL, Cabral V, Navati M, Doerner J, Charafeddine RA, *et al.* Curcumin-encapsulated nanoparticles as innovative antimicrobial and wound healing agent. *Nanomed Nanotechnol Biol Med.* 2015;11(1):195–206. doi: <http://dx.doi.org/10.1016/j.nano.2014.09.004>
- Mohanty C, Sahoo SK. Curcumin and its topical formulations for wound healing applications. *Drug Discov Today.* 2017;22(10):1582–92. doi: <http://dx.doi.org/10.1016/j.drudis.2017.07.001>
- Gupta SC, Patchva S, Aggarwal BB. Therapeutic roles of curcumin: Lessons learned from clinical trials. *AAPS J.* 2013;15(1):195–218.
- Liu Y, Cai Y, Jiang X, Wu J, Le X. Molecular interactions, characterization and antimicrobial activity of curcumin-chitosan blend films. *Food Hydrocoll.* 2016;52:564–72. doi: <http://dx.doi.org/10.1016/j.foodhyd.2015.08.005>
- Luo N, Varaprasad K, Reddy GVS, Rajulu AV, Zhang J. Preparation and characterization of cellulose/curcumin composite films. *RSC Adv.* 2012;2(22):8483–8.
- Govindaraj P, Kandasubramanian B, Kodam KM. Molecular interactions and antimicrobial activity of curcumin (*Curcuma longa*) loaded polyacrylonitrile films. *Mater Chem Phys.* 2014;147(3):934–41. doi: <http://dx.doi.org/10.1016/j.matchemphys.2014.06.040>
- Li X, Nan K, Li L, Zhang Z, Chen H. *In vivo* evaluation of curcumin nanoformulation loaded methoxy poly(ethylene glycol)-graft-chitosan composite film for wound healing application. *Carbohydr Polym.* 2012;88(1):84–90. doi: <http://dx.doi.org/10.1016/j.carbpol.2011.11.068>
- Thomas P, Duolikun T, Rumjit NP, Moosavi S, Lai CW, Bin Johan MR, *et al.* Comprehensive review on nanocellulose: recent developments, challenges and future prospects. *J Mech Behav Biomed Mater.* 2020;110:103884. doi: <https://doi.org/10.1016/j.jmbbm.2020.103884>
- Moohan J, Stewart SA, Espinosa E, Rosal A, Rodríguez A, Larrañeta E, *et al.* Cellulose nanofibers and other biopolymers for biomedical applications. a review. *Appl Sci.* 2019;10(1):65. doi: <https://doi.org/10.3390/app10010065>
- Trache D, Tarchoun AF, Derradji M, Hamidon TS, Masruchin N, Brosse N, *et al.* Nanocellulose: from fundamentals to advanced applications. *Front Chem.* 2020;8:392. doi: <https://doi.org/10.3389/fchem.2020.00392>
- Jorfi M, Foster EJ. Recent advances in nanocellulose for biomedical applications. *J Appl Polym Sci.* 2015;132(14):1–19. doi: <https://doi.org/10.1002/app.41719>
- Khalid MY, Al Rashid A, Arif ZU, Ahmed W, Arshad H. Recent advances in nanocellulose-based different biomaterials: types, properties, and emerging applications. *J Mater Res Technol.* 2021;14:2601–23. doi: <https://doi.org/10.1016/j.jmrt.2021.07.128>
- Lin N, Dufresne A. Nanocellulose in biomedicine: current status and future prospect. *Eur Polym J.* 2014;59:302–25. doi: <http://dx.doi.org/10.1016/j.eurpolymj.2014.07.025>
- Das S, Ghosh B, Sarkar K. Nanocellulose as sustainable biomaterials for drug delivery. *Sensors Int.* 2022;3:100135. doi: <https://doi.org/10.1016/j.sintl.2021.100135>

32. Zikmundova M, Vereshaka M, Kolarova K, Pajorova J, Svorcik V, Bacakova L. Effects of bacterial nanocellulose loaded with curcumin and its degradation products on human dermal fibroblasts. *Materials*. 2020;13(21):4759. doi: <https://doi.org/10.3390/ma13214759>
33. Gunathilake TMSU, Ching YC, Uyama H, Hai ND, Chuah CH. Enhanced curcumin loaded nanocellulose: a possible inhalable nanotherapeutic to treat COVID-19. *Cellulose*. 2022;29(3):1821–40. doi: <https://doi.org/10.1007/s10570-021-04391-8>
34. Wan S, Sun Y, Qi X, Tan F. Improved bioavailability of poorly water-soluble drug curcumin in cellulose acetate solid dispersion. *Aaps Pharm*. 2021;13:159–66. doi: <https://doi.org/10.1208/s12249-011-9732-9>
35. El-Nashar DE, Rozik NN, Soliman AM, Helaly F. Study the release kinetics of curcumin released from PVA/curcumin composites and its evaluation towards hepatocarcinoma. *Jf Appl Pharm Sci*. 2016;6(7):067–072. doi: <https://doi.org/10.7324/JAPS.2016.60710>
36. Ching YC, Gunathilake TMS, Chuah CH, Ching KY, Singh R, Liou NS. Curcumin/Tween 20-incorporated cellulose nanoparticles with enhanced curcumin solubility for nano-drug delivery: characterization and in vitro evaluation. *Cellulose*. 2019;26:5467–81. doi: <https://doi.org/10.1007/s10570-019-02445-6>
37. Naz S, Ali JS, Zia M. Nanocellulose isolation characterization and applications: a journey from non-remedial to biomedical claims. *Bio-Design Manuf*. 2019;2(3):187–212. doi: <https://doi.org/10.1007/s42242-019-00049-4>
38. Nasution H, Harahap H, Al Fath MT, Afandy Y. Physical properties of sago starch biocomposite filled with nanocrystalline cellulose (NCC) from rattan biomass: the effect of filler loading and co-plasticizer addition. *IOP Conf Ser Mater Sci Eng*. 2018;309(1):012033.
39. Burhani D, Septevani AA. Isolation of nanocellulose from oil palm empty fruit bunches using strong acid hydrolysis. *AIP Conf Proc*. 2018; 020005. doi: <https://doi.org/10.1063/1.5064291>
40. Lubis MF, Hasibuan PAZ, Syahputra H, Astyka R, Baruna I. Phytochemical profile and pharmacological activity of *Vernonia amygdalina* delile stem bark extracts using different solvent extraction. *OAMJMS*. 2022;10:860–6.
41. Phanthong P, Guan G, Ma Y, Hao X, Abudula A. Effect of ball milling on the production of nanocellulose using mild acid hydrolysis method. *J Taiwan Inst Chem Eng*. 2016;60:617–22. doi: <http://dx.doi.org/10.1016/j.jtice.2015.11.001>
42. Guo Y, Zhang Y, Zheng D, Li M, Yue J. Isolation and characterization of nanocellulose crystals via acid hydrolysis from agricultural waste-tea stalk. *Int J Biol Macromol*. 2020;163:927–33. doi: <https://doi.org/10.1016/j.ijbiomac.2020.07.009>
43. Leisyah BM. The effect of antioxidant of grapeseed oil as skin anti-aging in nanoemulsion and emulsion preparations. *Rasayan J Chem*. 2019;12(3):1185–94.
44. Tong WY, Bin Abdullah AYK, Binti Rozman NAS, Bin Wahid MIA, Hossain MS, Ring LC, *et al.* Antimicrobial wound dressing film utilizing cellulose nanocrystal as drug delivery system for curcumin. *Cellulose*. 2018;25(1):631–8. doi: <https://doi.org/10.1007/s10570-017-1562-9>
45. Taher MA, Zahan KA, Rajaie MA, Ring LC, Rashid SA, Mohd Nor Hamin NS, *et al.* Nanocellulose as drug delivery system for honey as antimicrobial wound dressing. *Mater Today Proc*. 2020;31:14–7. doi: <https://doi.org/10.1016/j.matpr.2020.01.076>
46. Siregar FK, Nasution DY, Muis Y, Kaban DY. Preparation and characterization of antibacterial film based on carboxymethylcellulose from gebang leaf (*Coryphantha*), polyvinyl alcohol and citric acid. *Rasayan J Chem*. 2019;12(2):554–64.
47. Morais JPS, Rosa MDF, De Souza Filho MDSM, Nascimento LD, Do Nascimento DM, Cassales AR. Extraction and characterization of nanocellulose structures from raw cotton linter. *Carbohydr Polym*. 2013;91(1):229–35. doi: <http://dx.doi.org/10.1016/j.carbpol.2012.08.010>
48. Dai H, Ou S, Huang Y, Huang H. Utilization of pineapple peel for production of nanocellulose and film application. *Cellulose*. 2018;25(3):1743–56. doi: <https://doi.org/10.1007/s10570-018-1671-0>
49. He H, Cai R, Wang Y, Tao G, Guo P, Zuo H, *et al.* Preparation and characterization of silk sericin/PVA blend film with silver nanoparticles for potential antimicrobial application. *Int J Biol Macromol*. 2017;104:457–64. doi: <http://dx.doi.org/10.1016/j.ijbiomac.2017.06.009>
50. O'Donnell KL, Oporto-Velasquez GS, Comolli N. Evaluation of acetaminophen release from biodegradable poly (Vinyl Alcohol) (PVA) and nanocellulose films using a multiphase release mechanism. *Nanomaterials*. 2020;10:301. doi: <https://doi.org/10.3390/nano10020301>
51. Anirudhan TS, Manjusha V, Sekhar VC. A new biodegradable nano cellulose-based drug delivery system for pH-controlled delivery of curcumin. *Int J Biol Macromol*. 2021;183:2044–54. doi: <https://doi.org/10.1016/j.ijbiomac.2021.06.010>
52. Sampath M, Lakra R, Korrapati P, Sengottuvelan B. Curcumin loaded poly (lactic-co-glycolic) acid nanofiber for the treatment of carcinoma. *Colloids Surf B Biointerf*. 2014;117:128–34. doi: <https://doi.org/10.1016/j.colsurfb.2014.02.020>
53. Sun W, Zou Y, Guo Y, Wang L, Xiao X, Sun R, *et al.* Construction and characterization of curcumin nanoparticles system. *J Nanopart Res*. 2014;6:2317. doi: <https://doi.org/10.1007/s11051-014-2317-2>
54. Solghi S, Emam-Djomeh Z, Fathi M, Farahani F. The encapsulation of curcumin by whey protein: assessment of the stability and bioactivity. *J Food Proc Eng*. 2020;43(6):e13403. doi: <https://doi.org/10.1111/jfpe.13403>
55. Zhu L, Feng L, Luo H, Dong R, Wang, M, Yao G, *et al.* Characterization of polyvinyl alcohol-nanocellulose composite film and its release effect on tetracycline hydrochloride. *Ind Crops Prod*. 2022;188:115723. doi: <https://doi.org/10.1016/j.indcrop.2022.115723>
56. Kolakovic R, Peltonen L, Laukkanen A, Hirvonen J, Laaksonen T. Nanofibrillar cellulose films for controlled drug delivery. *Eur J Pharm Biopharm*. 2012;82:308–15. doi: <https://doi.org/10.1016/j.ejpb.2012.06.011>
57. Yuan Y, Zhang S, Ma M, Wang D, Xu Y. Encapsulation and delivery of curcumin in cellulose nanocrystals nanoparticles using pH-driven method. *LWT*. 2022;155:112863. doi: <https://doi.org/10.1016/j.lwt.2021.112863>
58. Varghese RT, Cherian RM, Chirayil CJ, Antony T, Kargazadeh H, Thomas S. Nanocellulose as an avenue for drug delivery applications: a mini-review. *J Compos Sci*. 2023;7:210. doi: <https://doi.org/10.3390/jcs7060210>
59. Ali M, Mahmood AH, Hussain S, Ahmed F. An investigation into the antibacterial properties of bamboo/cotton blended fabric and potential limitations of the test method AATCC 147. *J Nat Fibers*. 2021;18(1):51–8. doi: <https://doi.org/10.1080/15440478.2019.1612305>
60. Balouiri M, Sadiki M, Ibsouda SK. Methods for *in vitro* evaluating antimicrobial activity: a review. *J Pharm Anal*. 2016;6(2):71–9. doi: <http://dx.doi.org/10.1016/j.jpha.2015.11.005>
61. Jabber LJY, Grumo JC, Alguno AC, Lubguban AA, Capangpangan RY. Influence of cellulose fibers extracted from pineapple (*Ananas comosus*) leaf to the mechanical properties of rigid polyurethane foam. *Mater Today Proc*. 2020;46:1735–9. doi: <https://doi.org/10.1016/j.matpr.2020.07.566>
62. Rigg-Aguilar P, Moya R, Oporto-Velasquez GS, Vega-Baudrit J, Starbird R, Puente-Urbina A, *et al.* Micro- and nanofibrillated cellulose (MNFC) from Pineapple (*Ananas comosus*) stems and their application on polyvinyl acetate (PVAc) and urea-formaldehyde (UF) wood adhesives. *J Nanomater*. 2020;1393160. doi: <https://doi.org/10.1155/2020/1393160>
63. Salimi S, Sotudeh-Gharebagh R, Zarghami R, Chan SY, Yuen KH. Production of nanocellulose and its applications in drug delivery: a critical review. *ACS Sustain Chem Eng*. 2019;7(19):15800–27. doi: <https://doi.org/10.1021/acssuschemeng.9b02744>

64. Kaur P, Sharma N, Munagala M, Rajkhowa R, Aallardyce B, Shastri Y, *et al.* Nanocellulose: resources, physio-chemical properties, current uses and future applications. *Front Nanotechnol.* 2021;3:1–17. doi: <https://doi.org/10.3389/fnano.2021.747329>
65. Yoon SY, Han SH, Shin SJ. The effect of hemicelluloses and lignin on acid hydrolysis of cellulose. *Energy [Internet].* 2014;77:19–24. Available from: <http://dx.doi.org/10.1016/j.energy.2014.01.104>
66. Chen G, Wang X, Jiang Y, Mu X, Liu H. Insights into the inhibition of acidic hydrolysis of cellulose by its solation. *ACS Sustain Chem Eng.* 2018;6(8):10999–1007. doi: <https://doi.org/10.1021/acssuschemeng.8b02418>
67. Hamzah AFA, Hamzah MH, Man HC, Jamali NS, Siajam SI, Ismail MH. Recent updates on the conversion of pineapple waste (*Ananas comosus*) to value-added products, future perspectives and challenges. *Agronomy.* 2021;11(11):2221. doi: <https://doi.org/10.3390/agronomy11112221>
68. Egot MP, Alguno AC. Preparation and characterization of cellulose acetate from pineapple (*Ananas comosus*) leaves. *Key Eng Mater.* 2018;772:8–12. doi: <https://doi.org/10.4028/www.scientific.net/KEM.772.8>
69. Pandi N, Sonawane SH, Anand Kishore K. Synthesis of cellulose nanocrystals (CNCs) from cotton using ultrasound-assisted acid hydrolysis. *Ultrason Sonochem.* 2021;70(May 2020):105353. doi: <https://doi.org/10.1016/j.ultsonch.2020.105353>
70. Tang Y, Yang S, Zhang N, Zhang J. Preparation and characterization of nanocrystalline cellulose via low-intensity ultrasonic-assisted sulfuric acid hydrolysis. *Cellulose.* 2014;21(1):335–46. doi: [10.1007/s10570-013-0158-2](https://doi.org/10.1007/s10570-013-0158-2)
71. Listyanda RF, Wildan MW, Ilman MN. Preparation and characterization of cellulose nanocrystal extracted from ramie fibers by sulfuric acid hydrolysis. *Heliyon.* 2020;6(11):e05486. doi: <https://doi.org/10.1016/j.heliyon.2020.e05486>
72. Sun B, Zhang M, Hou Q, Liu R, Wu T, Si C. Further characterization of cellulose nanocrystal (CNC) preparation from sulfuric acid hydrolysis of cotton fibers. *Cellulose.* 2016;23(1):439–50. doi: <https://doi.org/10.1007/s10570-015-0803-z>
73. Chen L, Wang Q, Hirth K, Baez C, Agarwal UP, Zhu JY. Tailoring the yield and characteristics of wood cellulose nanocrystals (CNC) using concentrated acid hydrolysis. *Cellulose.* 2015;22(3):1753–62. <https://doi.org/10.1007/s10570-015-0615-1>
74. Kumar A, Singh Negi Y, Choudhary V, Kant Bhardwaj N. Characterization of cellulose nanocrystals produced by acid-hydrolysis from sugarcane bagasse as agro-waste. *J Mater Phys Chem.* 2020;2(1):1–8. doi: <https://doi.org/10.12691/jmpc-2-1-1>
75. Fan B, Chen S, Yao Q, Sun Q, Jin C. Fabrication of cellulose nanofiber/AlOOH aerogel for flame retardant and thermal insulation. *Materials (Basel).* 2017;10(3):1–10. doi: <https://doi.org/10.3390/ma10030311>
76. Song S, Liu Z, Abubaker MA, Ding L, Zhang J, Yang S, *et al.* Antibacterial polyvinyl alcohol/bacterial cellulose/nano-silver hydrogels that effectively promote wound healing. *Mater Sci Eng C.* 2021;126:112171. doi: <https://doi.org/10.1016/j.msec.2021.112171>
77. Nam S, French AD, Condon BD, Concha M. Segal crystallinity index revisited by the simulation of X-ray diffraction patterns of cotton cellulose I β and cellulose II. *Carbohydr Polym.* 2016;135:1–9. doi: <http://dx.doi.org/10.1016/j.carbpol.2015.08.035>
78. Rashid S, Dutta H. Characterization of nanocellulose extracted from short, medium and long grain rice husks. *Ind Crops Prod.* 2020;154:112627. doi: <https://doi.org/10.1016/j.indcrop.2020.112627>
79. Jordan JH, Easson MW, Dien B, Thompson S, Condon BD. Extraction and characterization of nanocellulose crystals from cotton gin motes and cotton gin waste. *Cellulose.* 2019;26(10):5959–79. doi: <https://doi.org/10.1007/s10570-019-02533-7>
80. Raju V, Revathiswaran R, Subramanian KS, Parthiban KT, Chandrakumar K, Anoop EV, *et al.* Isolation and characterization of nanocellulose from selected hardwoods, viz., *Eucalyptus tereticornis* Sm. and *Casuarina equisetifolia* L., by steam explosion method. *Sci Rep.* 2023;13(1):1–15. doi: <https://doi.org/10.1038/s41598-022-26600-5>
81. Mondal S. Review on nanocellulose polymer nanocomposites. *Polym Plast Technol Eng.* 2018;57(13):1377–91. doi: <https://doi.org/10.1080/03602559.2017.1381253>
82. El-Shamy AG, Attia W, Abd El-Kader KM. The optical and mechanical properties of PVA-Ag nanocomposite films. *J Alloys Compd.* 2014;590:309–12. doi: <http://dx.doi.org/10.1016/j.jallcom.2013.11.203>
83. Korhonen K, Granqvist N, Ketolainen J, Laitinen R. Monitoring of drug release kinetics from thin polymer films by multi-parametric surface plasmon resonance. *Int J Pharm.* 2015;494(1):531–6. doi: <http://dx.doi.org/10.1016/j.ijpharm.2015.08.071>
84. Wong RSH, Dodou K. Effect of drug loading method and drug physicochemical properties on the material and drug release properties of poly (ethylene oxide) hydrogels for transdermal delivery. *Polymers (Basel).* 2017;9(7):286. doi: <https://doi.org/10.3390/polym9070286>
85. Souto EB, Baldim I, Oliveira WP, Rao R, Yadav N, Gama FM, *et al.* SLN and NLC for topical, dermal, and transdermal drug delivery. *Expert Opin Drug Deliv.* 2020;17(3):357–77. doi: <https://doi.org/10.1080/17425247.2020.1727883>
86. Pinto RJB, Lameirinhas NS, Guedes G, da Silva GHR, Oskoei P, Spirk S, *et al.* Cellulose nanocrystals/chitosan-based nanosystems: synthesis, characterization, and cellular uptake on breast cancer cells. *Nanomaterials.* 2021;11(8):2057. doi: <https://doi.org/10.3390/nano11082057>
87. Chen H, Ye Z, Sun L, Li X, Shi S, Hu J, *et al.* Synthesis of chitosan-based micelles for pH responsive drug release and antibacterial application. *Carbohydr Polym.* 2018;189:65–71. doi: <https://doi.org/10.1016/j.carbpol.2018.02.022>
88. Zheng D, Huang C, Huang H, Zhao Y, Khan MRU, Zhao H, *et al.* Antibacterial mechanism of curcumin: a review. *Chem Biodivers.* 2020;17(8):e2000171. doi: <https://doi.org/10.1002/cbdv.202000171>
89. Lubis MF, Kaban VE, Aritonang JO, Satria D, Mulina AA, Febriani H. Acute toxicity and antifungal activity of the ointment *Murraya koenigii* ethanol extract. *Rasayan J Chem.* 2022;15(1):256–61. doi: <http://dx.doi.org/10.31788/RJC.2022.1516401>
90. Zorofchian Moghadamtousi S, Abdul Kadir H, Hassandarvish P, Tajik H, Abubakar S, Zandi K. A review on antibacterial, antiviral, and antifungal activity of curcumin. *Biomed Res Int.* 2014;2014:186864. doi: <https://doi.org/10.1155/2014/186864>
91. Whitley KD, Jukes C, Tregidgo N, Karinou E, Almada P, Cesbron Y, *et al.* FtsZ treadmilling is essential for Z-ring condensation and septal constriction initiation in *Bacillus subtilis* cell division. *Nat Commun.* 2021;12(1):2448. doi: <http://dx.doi.org/10.1038/s41467-021-22526-0>
92. Morão LG, Polaquini CR, Kopacz M, Torrezan GS, Ayusso GM, Dilari G, *et al.* A simplified curcumin targets the membrane of *Bacillus subtilis*. *Microbiologopen.* 2019;8(4):1–12. doi: <https://doi.org/10.1002/mbo3.683>
93. Dai C, Lin J, Li H, Shen J, Shen Z, Wang Y, *et al.* The natural product curcumin as an antibacterial agent: current achievements and problems. *Antioxidants.* 2022;11(3):459. doi: <https://doi.org/10.3390/antiox11030459>

How to cite this article:

Sumaiyah S, Hasibuan PAZ, Syahputra H, Lubis MF. The nanocrystalline cellulose from *Ananas comosus* leaf wastes: An overview to extraction, purification, and applications as curcumin drug delivery system. *J Appl Pharm Sci.* 2024;14(12):165–173.